

SEDIMENT FLUX ESTIMATES DERIVED FROM DIFFERENT INSTRUMENTS. T. N. Titus¹, ¹U.S. Geological Survey Astrogeology Science Center, 2255 North Gemini Dr., Flagstaff, AZ 86001, USA. (ttitus@usgs.gov)

Introduction: Dune fields are ubiquitous across the Solar System [1] with notable concentrations on Venus, Earth, Mars, and Titan. Dune fields on Earth and Mars are known to be active, suggesting the movement of sediment. While sediment flux estimates have been conducted based on analysis of dune migration rates measured from orbit, these estimates do not include sediment flux of flow-through sediment [2]. Flow through sediment flux (hereafter called SF) have only been measured on Earth but should be measured on other planets too. This necessitates in situ surface data collection.

Motivation: Over the past decade, a concerted effort has been made to measure SF at a Mars analog site using a range of instruments [3,4]. The aim was to identify a potential suite of instruments that could be sent to the surface of Mars.

Analog Site: The Grand Falls Dune Field (GFDF), located on the Navajo Nation a few kilometers from Grand Falls, is considered a Mars analog site due to the bimodal composition of the sediment, which includes a large fraction of basaltic grains [3].

Data Collected: Between 2013 and 2019, SF was measured downwind from an active barchan. Data collected included wind speed and sediment flux at three above ground level (AGL) and a single piezo-electric saltation sensor (SS) monitored particle counts and kinetic energy near the surface. In 2017, five additional SSs were added as a vertically placed array, approximately corresponding to the range of heights of the sediment catchers and anemometers. For calibration, we use the entire data collection from March 29-31, 2017. For analysis, we focus on a single short duration SF event (as determined by significant increases in sediment captured) that occurred March 30, 2017.

Table 1: Weighing BSNE Calibration Data.

	AGL (m)	Bulk Mass (kg)	Bulk Mass per Area (kg/m ²)	Volt Range (V)	Calibration (kg/m ² /V)
1	0.19	0.4899	554	0.827	670
2	0.50	0.1274	142	0.133	1064
3	1.01	0.0399	44.3	0.070	633

Weighing Sediment Catchers: Most sediment catchers only provide an estimate of bulk sediment flux as the timing of sediment collection is not precisely known. To overcome this, we used “weighing” Big Springs Number Eight (wBSNE) catchers that provide real-time sediment mass estimates using a load cell. The output is in voltage which is converted to mass by

comparing the range of voltage to the final amount of sediment mass collected. The sediment mass collected needs to be corrected for wBSNE sampling area (0.02 m x 0.05 m [5] and efficiency (0.9 [6]). Table 1 shows the heights and calibration coefficients. Fig. 1 shows calibrated data collected for the SF event.

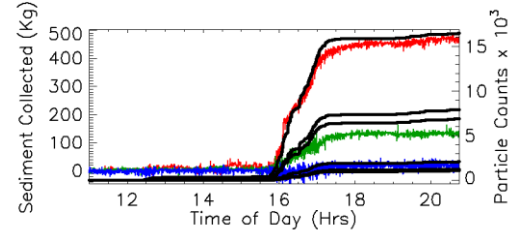


Figure 1: wBSNE accumulation of mass over a few hours. Red, green, and blue lines correspond to sensors 1 through 3, respectively. The black lines are raw particle counts from the six SSs. The heights are shown in Tables 1 and 2.

Table 2: Saltation sensor total particle count density, interpolated total sediment mass for sensor heights and corresponding estimated particle mass over the multi-day collection period.

Sensor	AGL (m)	Total Particle Cnt/Area (x10 ⁷ m ⁻²)	Est. Sed. Mass/Area (kg/m ²)	Est. Particle Mass (mg)
1	0.121	5.215	774.3	14.85
2	0.171	2.505	600.3	23.96
3	0.355	2.170	263.1	12.13
4	0.527	0.652	140.0	21.48
5	0.724	0.329	80.0	24.29
6	0.927	0.392	53.9	13.77

Saltation sensors: A total of six SensitTM saltation sensors were used. The heights and total number of particles counted for the data collection period are found in Table 2. The area sensitive to particle impacts is ~23.5 mm x ~13.5 mm. The wBSNEs were not exactly at the same elevation as the SSs, so we estimated the effective total mass that was detected by fitting an exponential quadratic equation: $m = \exp(a + bz + cz^2)$, where m is the mass/area and z is the corresponding height. Once the estimated sediment mass was calculated, we estimated the effective particle mass by dividing the mass/area by the total number of particles counted per unit area (Table 2). The estimated particle mass estimates do not consistently produce a smooth curve as a function of height. This may be due to GFDF having a bimodal composition of grains with different grain sizes and densities. This hypothesis should be

tested in dune fields where the grains are unimodal in size and composition.

Anemometers: The anemometers were used at similar heights to the wBSNEs to allow for direct comparison between wind speeds and sediment collected. A wind vane was used to determine wind direction.

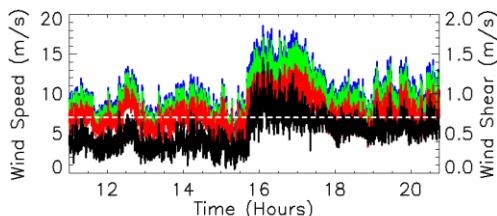


Figure 2: Wind speed and shear. The blue, green, and red lines show wind speeds at 1.05 m, 0.61 m, and 0.21 m, respectively. The black line is the calculated wind shear, u^* . The dashed horizontal line shows the value of 0.7 m/s, which is the value used for the shear threshold.

Data Analysis: Each individual data set can be used to characterize aspects of a SF event. Collectively, a comprehensive understanding can be developed.

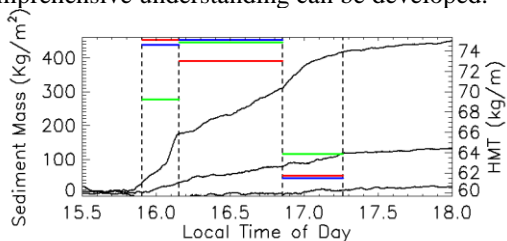


Figure 3: Comparison of three estimates for HMT for three time intervals using the wBSNE data. Red uses method 1. Green uses method 2. Blue uses method 3.

Sediment Flux: Each sediment catcher provides an estimate of the horizontal mass flux (HMF) at that height. To determine the horizontal mass transport (HMT), we must “integrate” over the HMF(z) from the ground to some upper height. Fig. 3 shows three periods of interest using three different methods to estimate HMT: (1) $\int_0^1 e^{a+bz+cz^2} dz$, (2) $\int_0^\infty e^{a+bz}$ using all three wBSNEs, and (3) using only the bottom two wBSNEs.

Saltation Flux: Using the particle mass estimates from Table 2, we estimated the HMT from the SSs. As opposed to the wBSNEs, the estimated HMFs have less noise and better fit an exponential decay, therefore we use method #2 (Table 3).

Table 3: Calculated HMT for three intervals during the saltation event. HMT calculated from three different fits as described in the text. HMT was also derived from the saltation sensors. The drift potential was scaled to the saltation sensors HMT estimates.

Time Interval		Time	HMT Calc. Method (kg/m)				
Start	End	(min)	wBSNEs #1	wBSNEs #2	wBSNEs #3	Saltation Method #2	Drift Potential
15.90	16.15	14.83	75.14	69.24	74.65	58.69	70.00
16.15	16.86	42.17	73.02	74.84	75.12	128.41	128.41

Particle Velocity Distribution: The SS also measure kinetic energy which can be converted to a normalized velocity by dividing by particle counts and mass. Estimated particle velocity peak at ~0.5 m AGL.

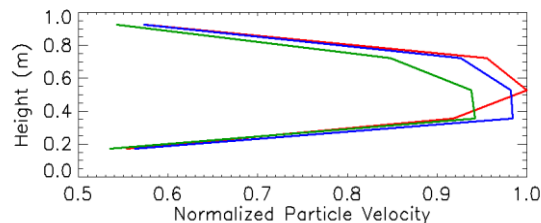


Figure 4: Saltation Sensor heights vs. normalized saltating particle velocity.

Drift Potential: The drift potential (DP) can be defined as $DP=C \underline{u}^2(u-u^*)$, where C is a constant, u is the wind shear, and u^* is the wind shear threshold for saltation. Table 3 shows the estimated HMT where $C=4.371 \text{ kg s}^3 \text{ m}^{-4}$ to scale the DP to the saltation estimates.

Discussion: The use of SSs to determine HMT is effective, can be used to characterize single events and is less noisy than wBSNEs, but requires that the particle mass can be independently determined. Additionally, estimate of particle velocity profiles can also be determined.

Acknowledgments: Fieldwork on the Navajo Nation was conducted under a permit from the Navajo Nation Minerals Department. Any persons wishing to conduct geologic investigations on the Navajo Nation must apply for and receive a permit from the Navajo Nation Minerals Department, P.O. Box 1910, Window Rock, Arizona 86515, telephone # (928) 871-6587.

The collection of the data used in this study was funded through a NASA PSTAR grant. The data can be downloaded from the USGS ScienceBase <https://doi.org/10.5066/P9IYGDGQ>.

Any use of trade, firm, or product names is for descriptive purposes only and does not imply endorsement by the U.S. Government.

References: [1] Lorenz R. & Zimbelman J. (2014) Dune Worlds: How windblown sand shapes planetary landscapes. Springer/Praxis, Chichester, UK, 308. [2] Sankey et al., 7IPDW, 3026. [3] Hayward et al. (2010) 2IPDW, 2004. [4] Titus et al. (2017) 5IPDW, 3008. [5] Fryrear (1986) *J. Soil Water Conserv.*, 41, 117. [6] Shao et al., (1993) *Aust. J. Soil Res.*, 31, 519.